Available online at www.sciencedirect.com
SCIENCE DIRECT®
Biochemical Pharmacology 65 (2003) 843–856
Biochemical Pharmacology
www.elsevier.com/locate/biochempharm

Statin effects on cholesterol micro-domains in brain plasma membranes

Christopher Kirsch, Gunter P. Eckert*, Walter E. Mueller

Department of Pharmacology, Biocenter Niederursel, University of Frankfurt, Marie-Curie-Str. 9, D-60439 Frankfurt, Germany

Received 15 October 2002; accepted 29 November 2002

Abstract

Recent epidemiological studies revealed inhibitors of the hydroxymethylglutaryl-coenzyme A reductase, so-called statins, to be effective in lowering the prevalence of Alzheimer's disease (AD). *In vitro*, statins strongly reduced the cellular amyloid beta-protein load by modulating the processing of the amyloid beta precursor protein. Both observations are probably linked to cellular cholesterol homeostasis in brain. So far, little is known about brain effects of statins. Recently, we could demonstrate that treatment of mice with the lipophilic compound lovastatin resulted in a discrete reduction of brain membrane cholesterol levels. To follow up these findings, we subsequently carried out a further *in vivo* study including lovastatin and simvastatin as lipophilic agents, as well as pravastatin as a hydrophilic compound, focussing on their efficiency to affect subcellular membrane cholesterol pools in synaptosomal plasma membranes of mice. In contrast to the hydrophilic pravastatin, the lipophilic lovastatin and simvastatin strongly reduced the levels of free cholesterol in SPM. Interestingly, lovastatin and pravastatin but not simvastatin significantly reduced cholesterol levels in the exofacial membrane leaflet. These changes were accompanied by modified membrane bulk fluidity. All three statins reduced the expression of the raft marker protein flotillin. Alterations in transbilayer cholesterol distribution have been suggested as the underlying mechanism that forces amyloidogenic processing of APP in AD. Thus, our data give some first insight in the mode of action of statins to reduce the prevalence of AD in clinical trials.

Keywords: Cholesterol; Statins; Lipids; Membrane; Alzheimer's disease; Brain

1. Introduction

Strong evidences indicate a functional link between increased Aβ generation and intracellular lipid metabolism during AD [1–10]. In this neurodegenerative disorder, extracellular Aβ plaques [11,12] are assumed to initiate cytotoxic effects via different signalling cascades that subsequently lead to synaptic loss and neuronal cell death [13–15]. However, the mechanisms linking neurodegeneration, Aβ production and cholesterol are only poorly understood [11,12].

The first hint that AD might be causally linked to altered lipid homeostasis came from the observation that the ε4 allele of the ApoE gene, encoding for an extracellular cholesterol-shuttle protein, is involved in the disease process [7]. Furthermore, statins, which are potent inhibitors of the HMG-CoA reductase and well-established peripheral cholesterol-lowering drugs [16], are discussed to exert some therapeutic potential in AD [17,18].

A retrospective epidemiological study recently demonstrated that long-term treatment of hypercholesterolaemic patients suffering CHD with lovastatin and pravastatin dramatically lowered the risk of developing AD compared to control subjects receiving other lipid-lowering medications [17]. Another epidemiological trial confirmed the possible effectiveness of pravastatin and of simvastatin in

* Corresponding author. Tel.: +49-69-79829378; fax: +49-69-79829374.
E-mail address: G.P.Eckert@em.uni-frankfurt.de (G.P. Eckert).

Abbreviations: Aβ, amyloid beta-protein; ACAT, acyl-coenzyme A-cholesterol acyltransferase; AD, Alzheimer's disease; ApoE, apolipoprotein E; APP, amyloid beta precursor protein; BBB, blood–brain barrier; CHD, coronary heart disease; CHO, Chinese hamster ovary; CHOD-PAP-method, cholesteroloxidase–peroxidase–aminophenazon–phenol-method; CSF, cerebrospinal fluid; DHE, dehydroergosterol; DPH, 1,6-diphenylhexa-1,3,5-triene; ER, endoplasmatic reticulum; HDL, high-density lipoprotein; HMG-CoA, hydroxymethylglutaryl-coenzyme A; LDL, low-density lipoprotein; MβCD, methyl-beta-cyclodextrin; NO, nitric oxide; NOs, nitric oxide synthase; PM, plasma membrane; POPC, 1-palmitoyl-2-oleylphosphatidylcholine; PUFA, polyunsaturated fatty acid; SDS, sodiumdodecylsulfate; SPM, synaptosomal plasma membrane; SREBP/SCAP, sterol regulatory element-binding protein/SREBP cleavage-activating protein complex; SUV, small unilamellar vesicle; TNBS, trinitrobenzensulfonic acid; VD, vascular dementia; VLDL, very low-density lipoprotein.

0006-2952/03/$ – see front matter © 2003 Elsevier Science Inc. All rights reserved.
doi:10.1016/S0006-2952(02)01654-4

lowering the prevalence of AD in hyperlipidaemic patients [18].

While simvastatin and lovastatin as lipophilic lactone pro-drugs [19] are assumed to affect the central nervous system by penetrating the BBB [20,21], pravastatin does not enter the brain [22]. In the periphery, pravastatin utilises active transport mechanisms for membrane passage [23]. Since the compound is undetectable in the CSF of healthy subjects [22], one might doubt that similar transport systems occur at the BBB. Thus, in face of current knowledge indicating a strict segregation of peripheral and cerebral cholesterol homeostasis [24] and an *in situ* brain cholesterol synthesis that completely satisfies cerebral demand [24], these findings suggest the existence of a signalling mechanism between peripheral and central lipid pools [25].

In vitro, cholesterol has been identified as an important parameter regulating the intracellular processing of the Aβ precursor APP [2–4,6]. Cholesterol depletion either induced with simvastatin and lovastatin as lipophilic inhibitors of the HMG-CoA reductase alone or in combination with MβCD induced a significant decrease in cellular Aβ load in hippocampal neurons [4,26]. This reduction in Aβ levels was accompanied by increased α-secretase activity [26], suggesting that membrane cholesterol variations are coupled with an activity shifting of APP-cleaving membrane-bound secretases [27–29]. Cholesterol depletion thereby possibly favours a non-raft lipid environment in which β- and γ-secretase cleavage of APP does not efficiently work [27–29]. Reversely, amyloidogenic processing of membranous APP is enhanced under conditions of high cellular cholesterol load [3]. This amyloidogenic-cleaving cascade is proposed to occur in cholesterol-rich functional lipid raft domains floating on the exofacial side of the membrane bilayer [27–29].

Regarding these *in vitro* findings, it seemed surprising that high-dosage treatment of guinea pigs with simvastatin *in vivo* led to strong reductions of $A\beta_{1-40}$ and $A\beta_{1-42}$ levels in brain homogenates *without* affecting total brain cholesterol levels [4]. Nevertheless, cholesterol precursor lathosterol in the brain was reduced significantly [4]. Diet-induced hypercholesterolaemia resulted in an accelerated brain amyloid pathology in a transgenic mouse model, which could be prevented by treatment with a peripheral cholesterol-lowering drug [30,31]. Again, peripheral diet barely affected cerebral cholesterol levels [30,31]. These findings indicate that the AD-related pharmacological effects of statins and other cholesterol-modulating agents in the brain may not be due to cholesterol-lowering effects within this compartment.

Actually, the beneficial potential of statins in hypercholesterolaemia as well as in CHD prevention trials [16,32,33] is not only attributed to their cholesterol-lowering properties [34–36]. Downstream blockage of isoprenoid synthesis might be the clue for *pleiotropic*, *non-lipid-related* statin effects [34–36]. These include i.e. direct anti-atherosclerotic properties like NOs-mediated restoration of endothelial dysfunction [34–36]. Such non-cholesterol effects seem to be more or less pronounced for all statin compounds [34–36] and might thus contribute to the differential neuroprotective potential of statins in clinical trials [17,18,37,38].

Furthermore, intracellular cholesterol homeostasis is subjected to different stringent regulating mechanisms, which keep the cellular cholesterol balance in an adjusted range [39,40]. HMG-CoA reductase as well as ACAT activity are under strict metabolic control of distinct feedback systems [39,40]. Other, mostly unknown mechanisms determine a non-uniform distribution of cholesterol and its derivatives within the cell [5,41]. It is suspected that any external impact on this cellular equilibrium, e.g. by statins, secondly induces metabolic shiftings within this system that are crucial for the observed pharmacological effects and probably imply cholesterol-independent lipid signalling cascades [34–36]. The possible relevance of such secondary effects is underlined by recent findings of Runz *et al.*, who demonstrated that subcellular cholesterol distribution highly affects presenilin localisation and cellular production of co-localised Aβ [42]. Reversely, Aβ itself was shown to alter cellular cholesterol distribution and cholesterol esterfication rate [43]. Beyond, intracellular ACAT activity and cholesterol ester levels were directly correlated with the generation of Aβ in CHO cells [44].

Recently, we could demonstrate that *in vivo* treatment of mice with the lipophilic compound lovastatin clearly affected the levels of free membrane cholesterol in the central nervous system [45]. Similar effects can be assumed for simvastatin, since high-dosage treatment with this compound induced a strong reduction of plasma 24*S*-hydroxycholesterol (cerebrosterol) levels in patients with hypercholesterolaemia [46]. Cerebrosterol mainly originates from the brain [47]. Herein we performed *in vivo* studies including lovastatin and simvastatin as lipophilic agents as well as pravastatin as a hydrophilic compound, focussing on their efficiency to affect bulk cholesterol levels and subdomain cholesterol distribution in SPM of mice. It was reported that SPM isolated from mice carrying the human ApoE 4 allele exhibit significant changes of the cholesterol transbilayer distribution [48]. Changes in membrane cholesterol distribution possibly represent a link between brain cholesterol homeostasis and the pathogenesis of AD.

2. Material and methods

2.1. Chemicals

Lovastatin and simvastatin were obtained from MSD Sharp & Dohme GmbH. Pravastatin was obtained from SANKYO PHARMA GmbH. Anti-flotillin IgG1 (catalogue no. F65020) and anti-Na^+/K^+-ATPase β2 (catalogue no. N69920) were purchased from Transduction Laboratories.

Peroxidase-conjugated anti-mouse IgG was purchased from Calbiochem. The enzyme kit for total cholesterol determination was obtained from Roche Diagnostics GmbH. HPLC-grade methanol and acetonitrile were obtained from Merck KGaA. All other chemicals and reagents were purchased from Sigma.

2.2. In vivo study design

Study design was adapted from [45]. Young (1 month) female C57BL/6J mice weighing from 16 to 21 g were used. All mice were obtained from the IFFA-CREDO S.A. Transgenic Alliance Department. The animals were tagged and housed in cages up to eight mice per cage under standard conditions with standard chow diet and water freely available during the study. In our experiments, mice were separately placed according to treatment. The total number of 92 mice were equally divided into a control and three statin groups receiving lovastatin, simvastatin or pravastatin, respectively. All experiments were carried out according to the guidelines of the Deutsches Tierschutzgesetz (BGBl 1998, Part I, No. 30, S. 1105 ff.) by individuals with appropriate training and experience.

Statin suspension was prepared as follows: Each day, 80 mg of each compound were suspended in 8 mL of a 0.2% (w/v) aqueous agarose gel giving a final concentration of 10 mg statin/mL. The suspension was homogenised and tempered in a water bath of 37° prior to treatment. Control treatment was prepared by simply tempering 8 mL of 0.2% (w/v) agarose gel (vehicle). Treatment was given once a day over a time period of 23 days by oral gavage via a pharyngeal tube (diameter: 1 mm) with a maximal application volume of 0.5 mL. Oral application was chosen as it is the standard administration of statins.

We applied statins at high doses within the upper range used in animal experiments [49] with the objective to detect even small pharmacological effects in the brain. Duration of treatment was estimated to be sufficient to detect statin-induced effects on brain cholesterol homeostasis [24,45]. Lovastatin- and pravastatin-treated mice received a suspension volume corresponding to a final concentration of 100 mg statin/kg b.wt. per day. As normal therapeutical dose of simvastatin is about one-half compared to lovastatin and pravastatin in humans, we decided to choose a dose of 50 mg statin/kg b.wt. per day in the simvastatin group. Mice were weighed daily for dose adjustment. Control mice received the same volume of 0.2% (w/v) agarose gel according to their weight. At the end of the study, 24 hr after the last treatment, mice were killed by decapitation. Blood was collected in tubes containing 0.05 mL heparin to avoid coagulation and centrifuged at 10,000 *g* and 4° for 10 min to gain the serum fraction. Brains were removed on ice and after dissection of the brainstem and the cerebellum the hemispheres were used for preparation of synaptosomes immediately. Cerebellum crude fraction was prepared according to [45].

2.3. Preparation of synaptosomes

Synaptosomes were prepared as previously described [50]. Shortly, 3–4 brains were homogenised in sucrose buffer for membrane preparation and centrifuged for 10 min at 585 *g* (4°). The supernatant was retained and the resulting pellet (P1) was re-homogenised and re-centrifuged. Combined supernatants were centrifuged for 10 min at 17,400 *g* (4°). The resulting pellet that contained synaptosomes and mitochondria (P2) was re-suspended and layered over a 7.5 and 14% ficoll solution (w/v). The gradients were centrifuged for 50 min at 87,300 *g* (4°). The material at the interface of the gradient was carefully removed.

2.4. TNBS labelling of synaptosomes

TNBS labelling was performed according to [51]. Briefly, synaptosomes were suspended in 5 mL of buffer IV (30 mmol/L NaCl, 120 mmol/L $NaHCO_3$, 11 mmol/L glucose, 1% (w/v) bovine serum albumin; pH 8.3) and divided into a control aliquot and a TNBS aliquot. The TNBS aliquot was incubated with TNBS (2 mmol/L) on ice at 4° (non-penetrating conditions) or at 37° (penetrating conditions) for 40 min. During that time, samples were sealed and darkened. Control aliquots were incubated analogously without TNBS. At 4°, TNBS covalently links the amino moieties of phospholipids from the exofacial leaflet [52] (Fig. 5A). At 37°, TNBS penetrates the core region of the membrane and trinitrophenylates both SPM leaflets [52]. Samples incubated under penetrating conditions thus indicate absolute quenching. After incubation time, the reaction was stopped by addition of 2.5 mL of 1% bovine serum albumin (w/v) in PBS-buffer (136.75 mmol/L NaCl, 2.68 mmol/L KCl, 6.48 mmol/L Na_2HPO_4, 1.47 mmol/L KH_2PO_4; pH 7.4). The samples were centrifuged for 15 min at 17,200 *g* (4°) in a JA-20 rotor using a Beckman J-2 centrifuge. The resulting pellets were suspended in 5 mL buffer I and layered over a 7.5 and 14% ficoll solution (w/v). The gradients were centrifuged for 50 min at 87,300 *g* (4°) in a SW-28 rotor using a Beckman L8-70M ultracentrifuge. The material at the interface of the gradient was carefully removed. After suspension with buffer I the interface material was centrifuged for 20 min at 48,000 *g* (4°) in a JA-20 rotor using Beckman J-2 centrifuge. The resulting synaptosomal pellets were re-suspended in buffer I and re-centrifuged analogously to remove remaining ficoll.

2.5. Preparation of SPM

SPM were prepared as previously described [50]. Briefly, control synaptosomes and TNBS-labelled synaptosomes were suspended in 15 mL buffer II (5 mmol/L Tris–HCl; pH 8.5). The synaptosomes were kept on ice for lysis for 1 hr and were vortexed rigorously every 15 min.

The suspension was centrifuged for 20 min at 43,000 *g* (4°). The pellet was re-suspended in 5 mL of ice-cold distilled water, laid on the top of 5 mL of sucrose gradient (0.9 mol/L sucrose, 10 mmol/L HEPES, 0.25 mmol/L EDTA; pH 7.4) and centrifuged for 40 min at 41,000 *g* (4°). SPM at the interface of the gradient were carefully removed, suspended in 5 mL of ice-cold water and centrifuged for 30 min at 48,000 *g* (4°). SPM pellets were suspended in 1 mL of PBS-buffer and stored in aliquots at −20°. The purity of the isolated membrane fraction was proved by marker enzyme assay. Freshly prepared SPM were marked by Western blotting analysis and the activity of Na^+/K^+-ATPase [50,53]. Marker enzyme protein and activity were significantly enriched in the SPM fraction (data not shown).

2.6. Preparation of SUVs

SUV were used as carrier vehicles for the incorporation of the fluorescent derivative DHE into SPM. The dynamic and stoichiometric exchange of native membrane cholesterol and DHE in unlabelled and TNBS-labelled sample preparations represents one basic principle in the research of transmembrane sterol distribution that has been described earlier [51,52]. DHE (from Sigma) was purified on a HPLC LiChrospher® 100 RP-18 column (diameter: 5 μm; length: 250 mm; from Merck, Germany) to approximately 99.9% purity using Varian Star equipment with a Rainin Dynamay solvent delivery system SD-200 and Varian Star 5.31 Chromatography Software (Varian Deutschland GmbH). The solvent system used was HPLC-grade acetonitrile:methanol 30:70 (v/v) at a flow rate of 1 mL/min. Samples were injected with a Varian Pro Star 410 auto sampler. The column eluant was monitored for absorbance at 215 nm using a Rainin Dynamax absorbance detector UV-D II. According to [51], HPLC-grade DHE (5 mmol/L in ethanol) was mixed with POPC (1 mg/mL in chloroform) in a molar ratio of 42/58 mol%. The mixture was evaporated under nitrogen and reduced pressure for 2 hr to yield a thin film. The film was dried for another 12 hr under nitrogen in the dark. Subsequently, 2 mL of buffer V (136.75 mmol/L NaCl, 2.68 mmol/L KCl, 8.1 mmol/L Na_2HPO_4, 1.47 mmol/L KH_2PO_4, 2 mg/mL glucose; pH 7.4) were added to the dried film. The suspension was vortexed for 1 min and then sonicated in a RK 510-H Sonorex bath sonicator (Bandelin Electronic). This procedure was repeated twice to yield a turbid mixture. The mixture was filled up to 4 mL with buffer V and then sonicated at 4° for 45 min with 40% duty cycle and output 2.5 (30% maximum power) using a B-15P Branson sonicator (Branson Ultrasonics Corp.). During sonication, nitrogen was blown slowly over the suspension. The suspension was then transferred to 3.5 mL polyallomer quick seal tubes (Beckman Coulter) and centrifuged for 1.75 hr at 140,000 *g* in a SW-41 rotor using a Beckman L8-70M ultracentrifuge. The upper half of the clear solution containing SUV was removed and stored under nitrogen at room temperature in the dark for further use.

2.7. DHE incorporation into SPM and determination of transbilayer cholesterol distribution

For the dynamic exchange of SPM cholesterol and liposomal DHE, both compounds were placed in the incubation medium in a 1:1 molar ratio [51,54]. DHE concentration in SUV was determined spectrometrically. One hundred microlitres of SUV preparation were mixed with 900 μL of water, 2 mL of Dole's reagent (2-propanol/heptane/water = 4/1/0.1) and 1 mL of heptane, vortex mixed for 30 s and centrifuged at 2000 *g* for 10 min at 4° in a Beckman GS-6R centrifuge. The upper heptane solution was dried under nitrogen in the dark and the dried film was dissolved in 500 μL of ethanol. An aliquot of this solution was filled up to 1 mL with water and its fluorescence intensity was measured at 37° in a SLM Luminescence Spectrometer Aminco-Bowman® Series 2 (SLM Aminco) using excitation and emission wavelengths of 324 and 375 nm, respectively. Equivalently, a standard curve for DHE in a concentration range from 0 to 100 μg/mL DHE was generated and used for the determination of total DHE amount per millilitre SUV preparation according to the fluorescence intensity signal.

SPM with and without TNBS (200 μg of protein, determined according to Lowry *et al.* [55]) were incubated with the appropriate volume of SUV solution and buffer V (total volume: 1 mL) for 1 hr at 37° and 1400 rpm in a thermomixer (Thermomixer comfort). Blanks were incubated without DHE. SPM were then centrifuged at 20,000 *g* and 4° for 15 min in a Beckman microfuge R. The pellet was washed once again with 0.5 mL buffer V and was re-centrifuged. SPM pellets were suspended in 1 mL of PBS-buffer and tempered at 37° for 1 min. Fluorescence intensity was directly measured in a SLM Luminescence Spectrometer Aminco-Bowman® Series 2 (Ex. 324 nm, Em. 375 nm; Fig. 5B). The detector signal was adjusted to 60% maximum photomultiplier voltage for the DHE loaded sample without TNBS. Blanks and TNBS-labelled preparations of the same sample were subsequently measured at same photomultiplier voltage.

2.8. Determination of SPM leaflet anisotropy

The experimental investigation of individual SPM leaflet structure is based on a method established by Schroeder *et al.* [56]. Plasma membranes are composed of cytofacial and exofacial membrane leaflets that predominantly differ in structure and fluidity because of an asymmetric transbilayer distribution of lipids. DPH is located near the hydrophobic core of the membrane and aligns axial to the fatty acid chains of membrane phospholipids [57]. It is equally distributed between both bilayer leaflets. The rotational flexibility of DPH within this membrane matrix

expressed as steady-state fluorescence anisotropy gives information on the surrounding of the lipid environment of the probe [58]. According to Weber [59], the determination of the individual DPH anisotropy values of both bilayer leaflets requires the simultaneous measuring of the DPH fluorescence intensity F and the steady-state fluorescence anisotropy r. In this binary system, both leaflets are not coupled and mathematically assumed to behave as different fluorescence compartments that are not equally accessible to TNBS [59–61], which finds its mathematical equivalent in Eq. (1) of additive fractional leaflet anisotropies.

$$r = \frac{F_c r_c}{F} + \frac{(F - F_c) r_e}{F}. \quad (1)$$

F and F_c are the fluorescence intensities of DPH obtained from SPM preparations pre-incubated without TNBS or with TNBS at 4°, respectively. The corresponding steady-state anisotropy values are described with r (total anisotropy) for untreated preparations and r_c (cytofacial leaflet anisotropy) for preparations pre-treated with TNBS at 4° (non-penetrating conditions). r_e as the exofacial leaflet anisotropy can be calculated from Eq. (1). Thereby, fluorescence anisotropy is inversely correlated with membrane fluidity [57,62].

Each parameter in (1) was individually determined for each preparation (TNBS-labelled and unlabelled). Therefore, 100 μL of SPM membrane suspension (protein concentration 30 μg/100 μL) were incubated with 900 μL PBS-buffer and 0.1 μL of a DPH stock solution (0.1 mg DPH/mL tetrahydrofurane) for 45 min at 37°. Blanks were incubated analogously without DPH. Steady-state anisotropy and fluorescence intensity were directly measured in a SLM Luminescence Spectrometer Aminco-Bowman® Series 2 using excitation and emission wavelengths of 360 and 450 nm (slits 4 nm), respectively. The detector signal was adjusted to 80% maximum photomultiplier voltage for the DPH loaded sample without TNBS. Blanks and TNBS-labelled preparations of the same sample were subsequently measured at same photomultiplier voltage.

2.9. Pyrene fluorescence measurements

The compact pyrene molecule is predominantly located in lipophilic regions in the deep membrane interior [63]. Pyrene diffuses laterally within the hydrocarbon core of the bilayer [63]. The intra-membranous interaction of two excited pyrene monomers results in the formation of defined excimers and consequently in the emission of discrete fluorescence light. Accordingly, the intensity of this fluorescence signal is equated with the lateral bulk fluidity capacities of the membrane.

Pyrene bulk fluorescence measurements were performed according to [45]. SPM membrane suspension was adjusted to a protein concentration of about 500 μg/mL with buffer III (Tris–HCl 5 mmol/L; pH 7.4). One hundred microlitres of membrane suspension were incubated with 900 μL of buffer III for 45 min at 37° in a water quench. After incubation time, 1 μL of a pyrene solution (1 mmol/L in dimethylformamide) was added. The suspension was vortexed rigorously and incubated for another minute at 37° after which time fluorescence intensity reached a maximum.

Fluorescence intensity was measured in a SLM Luminescence Spectrometer Aminco Bowman® Series 2 using an excitation wavelength of 334 nm for the determination of bulk fluorescence. In the recorded emission scans, the fluorescence intensities of pyrene excimers and monomers at a wavelength of 482 and 373 nm, respectively, were noted. In each case, the ratio of excimer to monomer fluorescence values was calculated, which is termed *bulk fluorescence*.

2.10. Western blotting analysis

Flotillin and Na^+/K^+-ATPase expression in SPM homogenate from control and statin-treated mice were determined using sodiumdodecylsulfate–polyacrylamide gel electrophoresis (SDS–PAGE) and Western blotting analysis [64]. Proteins (40 μg) were transferred onto polyvinylidene difluoride (PVDF) membranes (Millipore) at constant amperage and subjected to Western blotting. The bound antibodies against flotillin (catalogue no. F65020) and Na^+/K^+-ATPase (catalogue no. N69920) were detected with a peroxidase-labelled secondary anti-mouse antibody using ECL reagents (Amersham Pharmacia Biotech). Quantification was performed using a densitometer and the Kodak DC1C software package.

2.11. Preparation of MβCD–cholesterol inclusion complexes

Inclusion complexes were prepared as earlier described [65]. In brief, cholesterol was re-crystallized with dichloromethane. Subsequently, an excess of crystalline cholesterol was suspended in 1 mL of a 30 mmol/L MβCD solution to gain saturated complexes. The suspension was incubated at 50° for 1 hr in a thermomixer at 1400 rpm. After this time, the preparation was centrifuged at 20,000 g at 4° for 10 min. The supernatant was centrifuged again and filtered through a Sartorius Minisart SRP 25 PTFE-membrane-filter (pore size 0.45 μm) to gain a clear solution. Cholesterol determination revealed a molar ratio for MβCD/cholesterol of 10/1. Complexes were used for cholesterol modulation immediately after preparation.

2.12. In vitro cholesterol modulation with MβCD and MβCD–cholesterol complexes

MβCD and MβCD–cholesterol complexes are valid tools for the modulation of cellular cholesterol values [2–4]. MβCD extracts cholesterol from the plasma membrane, whereas MβCD–cholesterol complexes operate as vesicular cholesterol donors [65].

For *in vitro* studies, middle-aged (10–12 months) female NMRI mice from Harlan-Winkelmann GmbH were used. Preparation of synaptosomes was performed as described above using eight brains at a time. Synaptosomal pellets were re-suspended in 20 mL of buffer I (0.32 mol/L sucrose, 10 mmol/L HEPES, 0.25 mmol/L EDTA; pH 7.4) and divided into two 10 mL aliquots. For cholesterol depletion, one aliquot was incubated with 1750 μL of buffer I and 250 μL of an aqueous MβCD-stock solution (400 mmol/L) giving a final MβCD-concentration of 8.3 mmol/L. For cholesterol enrichment, one aliquot was treated with 8 mL of the freshly prepared MβCD–cholesterol complex solution (final concentration 1.3 mmol cholesterol/L). Control aliquots were treated with buffer I only. The samples were vortex mixed and incubated for 30 min at 37° in a water quench. Subsequently, samples were centrifuged for 15 min at 48,000 *g* (4°) and the resulting pellets were re-washed in buffer I and re-centrifuged again. Pellets were then dissolved in 5 mL of buffer IV and labelled with TNBS. SPMs were prepared as described above.

2.13. Cholesterol determination

Free cholesterol was determined according to the CHOD-PAP-method with a special enzyme kit developed in our laboratory. In brief, the protocol of Auerbach *et al.* [66] was slightly modified by using 0.5% (w/v) MβCD in combination with Brij 35 as an 15% (w/v) aqueous solution to amplify the extraction of free cholesterol from membrane material with the aim to increase the sensitivity of the test. Cholesterol values were measured as triplicates after 2 hr of incubation at a wavelength of 490 nm in a micro plate reader (DigiScan, ASYS Hitech GmbH). The method was proofed to give valid and reproducible results [45,50,65].

Total cholesterol determination was performed with the cholesterol kit CHOL no. 2016630 from Roche Diagnostic GmbH using the CHOD-PAP-method.

2.14. Determination of total phospholipid content

Phospholipids were determined according to Chalvardjian and Rudnicki [67]. SPM (attuned to 50 μg protein) were extracted with 1 mL of chloroform/methanol 2:1 (v/v) for 5 min at 25° and 1400 rpm in a thermomixer. The turbid emulsion was centrifuged at 580 *g* and 4° for 5 min in a Beckman microfuge R. An amount of 0.5 mL of the organic phase were removed and evaporated in a block heater at 100°. After cooling down, 50 μL of perchloric acid were added and the liberation of organic phosphorus was accomplished by setting the heating elements to 180° for 15 min. After the tubes were cooled, 150 μL of distilled water were added followed by 1 mL of ammonium molybdate malachite green reagent (1 volume of 4.2% (w/v) ammonium molybdate and 3 volumes of 0.2% (w/v) malachite green in water, mixed for 30 min) and 40 μL of a 1.5% (w/v) aqueous solution of Tween 20. A standard curve for 0–10 μg phosphorus/mL was generated analogously. Blanks were carried throughout the procedure. Triplicates of samples, blanks and standards were measured without delay at a wavelength of 620 nm in a micro plate reader (DigiScan, ASYS Hitech GmbH).

2.15. Statistics

Statistical analysis was performed by one-way ANOVA combined with the Bonferroni post hoc test or the unpaired *t*-test. Correlations were performed according to Pearson using GraphPad Prism 3.0 software package.

3. Results

3.1. Statin effects on SPM cholesterol levels

Tissue cholesterol levels were measured in SPM and cerebelli as well as in the peripheral serum fraction.

Lovastatin, simvastatin and pravastatin exert different effects on SPM cholesterol levels in mice (Fig. 1A, Table 1). Lovastatin and simvastatin significantly reduce

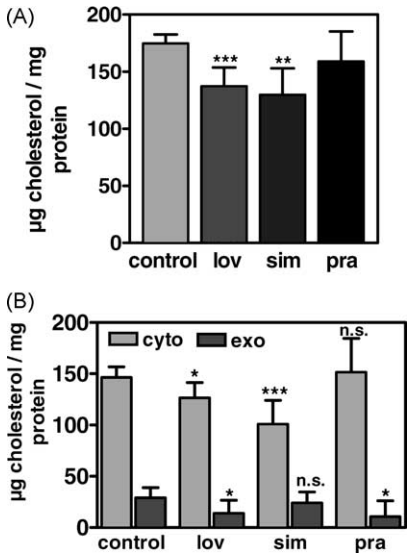

Fig. 1. Total levels and transbilayer distribution of unesterfied membrane cholesterol in SPM of control and statin-treated mice. (A) Levels of unesterfied cholesterol were determined in SPM of control and statin-treated C57BL/6J mice according to the CHOD-PAP-method (refer to Section 2). Data are means ± SD (N = 5–6). Statistical significance was estimated by one-way ANOVA combined with Bonferroni's multiple comparison post hoc test. (**) $P < 0.01$, (***) $P < 0.001$ significant vs. control. lov, lovastatin; sim, simvastatin; pra, pravastatin. (B) Cytofacial (cyto) and exofacial (exo) leaflet cholesterol (CHOL) levels were determined in SPM of control and statin-treated C57BL/6J mice (lov, lovastatin; sim, simvastatin; pra, pravastatin). Synaptosomes were labelled according to the TNBS-quenching technique. Native SPM cholesterol was exchanged by SUV-incorporated DHE (refer to Section 2). Data are means ± SD (N = 5–6). (n.s.): not significant, (*) $P < 0.05$, (***) $P < 0.001$ significant vs. control value of the same leaflet (ANOVA).

Table 1
Total cholesterol and cholesterol ester levels in SPM and serum of control and statin-treated mice

	SPM		Serum total cholesterol (mg/dL)
	Total cholesterol (μg/mg protein)	Cholesterol ester (μg/mg protein)	
Control	204.30 ± 22.27	25.95 ± 28.86	43.96 ± 3.64
Lovastatin	184.50 ± 23.02	42.12 ± 22.92	49.46 ± 6.11
Simvastatin	181.90 ± 12.81	45.31 ± 27.77	49.34 ± 6.90
Pravastatin	178.50 ± 18.24	24.01 ± 33.25	52.76 ± 12.41

Cholesterol levels in SPM and serum of control and statin-treated C57BL/6J mice were determined enzymatically according to the CHOD-PAP-method (refer to Section 2). Statin-treated animals received 100 mg/kg b.wt. lovastatin or pravastatin and 50 mg/kg b.wt. simvastatin, respectively. Controls received vehicle only. Data are means ± SD (N = 5–6). ANOVA analysis revealed no statistical differences over all groups of treatment for each parameter determined.

free membrane cholesterol levels of about 20% (Fig. 1A). Pravastatin reduces free cholesterol on the average by 13%, but this reduction does not reach statistical significance (Fig. 1A). The reduction of brain cholesterol observed in our experiments of about 20% suggests effects on brain cholesterol *de novo* synthesis, since only 10–15% would be needed to compensate for the cholesterol efflux out of the brain, which seems to take pace at a daily rate of about 0.45% of total brain cholesterol [24]. Interestingly, all three statins reduce total membrane cholesterol, which comprises free and esterfied cholesterol, by about 10% (Table 1), although this effect does not reach statistical significance. Accordingly, lovastatin and simvastatin slightly enhance the amount of membranous cholesterol esters (Table 1).

We further investigated whether statin treatment affects SPM total phospholipid content expressed as μmol phosphorus/mg protein. No significant difference was observed between all groups (ANOVA). The respective mean ± SD values (N = 5–6) are 0.739 ± 0.140 for the control group, 0.602 ± 0.111 for the lovastatin group, 0.683 ± 0.140 for the simvastatin group and 0.733 ± 0.138 for the pravastatin group.

Interestingly, free cholesterol content in the cerebellum remains unaffected under statin treatment (data not shown), which confirms earlier findings [45].

Total cholesterol levels in serum of statin-treated mice are even slightly, although not significantly enhanced compared to control animals (Table 1), which might be explained by a compensatory peripheral over-expression of the HMG-CoA reductase enzyme [68]. Moreover, mice carry cholesterol mainly in the HDL fraction and have low LDL and VLDL cholesterol levels [68]. However, our findings are in agreement with several other reports in the mouse [45,68].

3.2. Validity of selective TNBS quenching

The determination of SPM individual leaflet anisotropy and sterol distribution requires the selective trinitrophenylation of the outer membrane leaflet under non-penetrating conditions (Fig. 5A). Since DPH distributes randomly in the bilayer [56], quenching values obtained at 4° should reach about one-half of maximum quenching, which is used as an indicator for the validity of the method. Mean ± SD values (N = 5–6) for percent quenching of DPH in the exofacial leaflet are 48.06 ± 3.38 in the control group, 46.06 ± 4.10 in the lovastatin group, 46.26 ± 2.51 in the simvastatin group and 48.48 ± 2.25 in the pravastatin group, respectively. Percent quenching does not statistically differ among all groups (ANOVA). These values are in good agreement with the calculated mole percent fractions of DPH in each leaflet [56]. TNBS incubation of synaptosomes under penetrating conditions (37°) results in DPH quenching values greater than 90% (data not shown), indicating that penetration of TNBS in the cytofacial leaflet was efficiently prevented at 4°.

3.3. Statin effects on SPM transbilayer cholesterol distribution

Cholesterol is not uniformly distributed within the PM [41,69]. About 7/10 of total membrane cholesterol are located within the cytofacial leaflet. Thereby, the ratio of exofacial to cytofacial cholesterol is not constant and increases, e.g. with age [51,54].

Consistent with previous findings [51], in young control mice approximately 85% of SPM cholesterol is located in the cytofacial membrane leaflet, whereas exofacial cholesterol accounts for about 15% of total SPM cholesterol (Fig. 1B). Pravastatin significantly reduces cholesterol content in the exofacial leaflet compared to untreated controls, whereas cytofacial cholesterol levels remain unaffected (Fig. 1B).

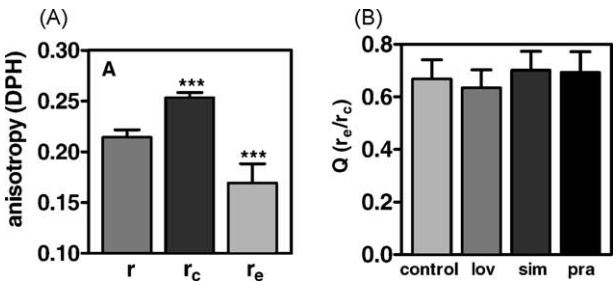

Fig. 2. DPH leaflet anisotropy values of SPM of control and statin-treated mice. Individual DPH leaflet anisotropy values as well as total SPM anisotropy values were determined in SPM of control and statin-treated C57BL/6J mice. Synaptosomes of control, lovastatin (lov)-, simvastatin (sim)- and pravastatin (pra)-treated mice were labelled according to the TNBS-quenching technique (refer to Section 2). (A) Total and individual leaflet DPH anisotropy values from SPM of control mice (r: total anisotropy, r_c: cytofacial leaflet anisotropy, r_e: exofacial leaflet anisotropy). Data are means ± SD (N = 5–6). (***) $P < 0.001$ significant vs. total anisotropy (t-test). (B) Ratios of exofacial (r_e) and cytofacial (r_c) anisotropy values were calculated for each group of treatment. ANOVA analysis revealed no statistical differences between all groups. Data are means ± SD (N = 5–6). According to (A), r_c values were significantly higher ((***) $P < 0.001$), r_e values significantly lower ((***) $P < 0.001$) compared to r values (t-test) in each group of treatment.

Similar to pravastatin, lovastatin also diminishes exofacial cholesterol levels. Significant cholesterol depletion also occurs in the cytofacial membrane leaflet compared to control mice (Fig. 1B).

Simvastatin-induced depletion of free membrane cholesterol predominantly occurs in the cytofacial membrane leaflet and only weakly affects exofacial membrane cholesterol levels (Fig. 1B).

3.4. Statin effects on DPH leaflet anisotropy

Anisotropy values of DPH are inversely correlated with the membrane fluidity in terms of acyl-chain flexibility [57].

In good agreement with earlier studies [51,54], DPH anisotropy values in the cytofacial membrane leaflet are significantly higher compared to the exofacial leaflet, which is exemplarily shown for membranes of placebo-treated control mice in Fig. 2A. Also, cytofacial leaflet anisotropy is significantly enhanced compared to total anisotropy values in all groups of treatment (data not shown).

Despite the cholesterol re-distribution effects of the statins (Fig. 1), Fig. 2B clearly illustrates that lovastatin, simvastatin and pravastatin treatment exerts no effect on individual DPH leaflet anisotropy values in SPM of mice. Ratio values of exofacial/cytofacial leaflet anisotropy are similar in all groups of treatment (Fig. 2B). Also total anisotropy values of SPM remain unaffected under statin

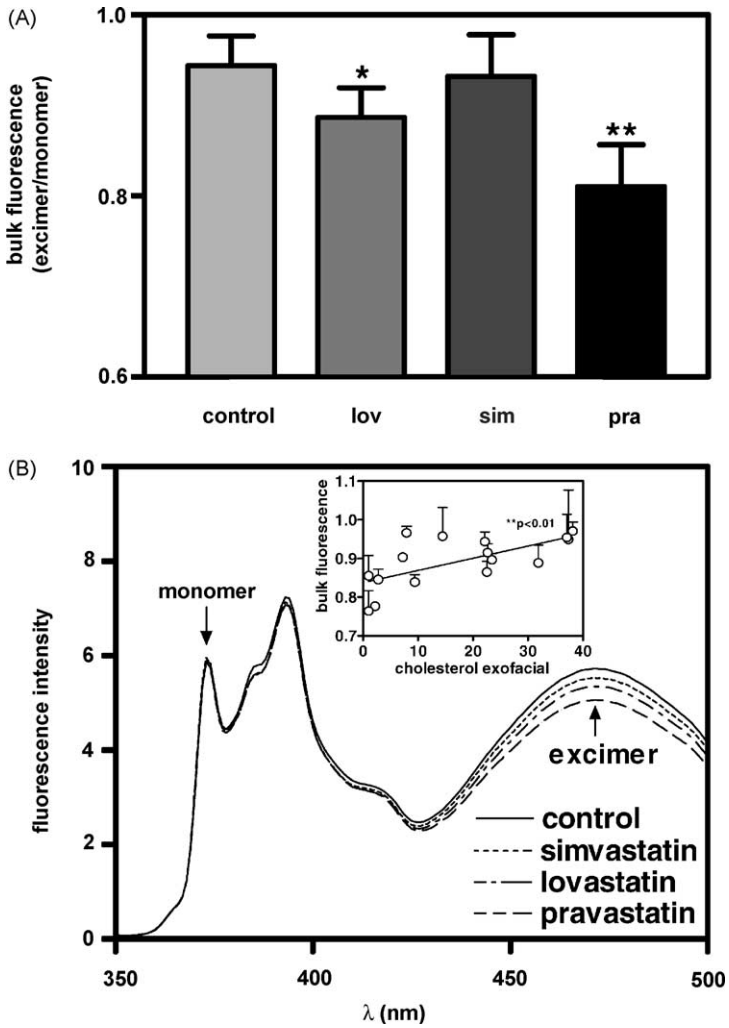

Fig. 3. Pyrene bulk fluorescence values of SPM of control and statin-treated mice. (A) Pyrene bulk fluorescence values of SPM of control and statin-treated C57BL/6J mice were measured (lov, lovastatin; sim, simvastatin; pra, pravastatin). The ratio of excimer to monomer fluorescence was used as a marker for the lateral mobility of the dye within the membrane hydrocarbon core. Data are means ± SD (N = 5–6). (∗) $P < 0.05$, (∗∗) $P < 0.01$ significant vs. control (ANOVA). (B) Averaged pyrene emission scans of pyrene bulk fluorescence measurements at an excitation wavelength of 334 nm are shown (see A). The fluorescence maximum of pyrene monomers occurs at 373 nm, while fluorescence emission of pyrene excimers occurs at approximately 480 nm. Pyrene bulk fluorescence is expressed as the intensity ratio of excimer to monomer fluorescence (F_e/F_m). Emission scans are shown for SPM of control and statin-treated mice. Data are means ± SD (N = 5–6). Each data point represents an average of three independent determinations. Inlet: exofacial leaflet cholesterol contents (μg/mg protein) of SPM of control and statin-treated mice were correlated with the corresponding pyrene bulk fluorescence values (see A). Data are means ± SD, N = 4–6; (∗∗) $P < 0.01$ significant correlation (Pearson). No significant correlation was apparent for cytofacial leaflet cholesterol contents (data not shown).

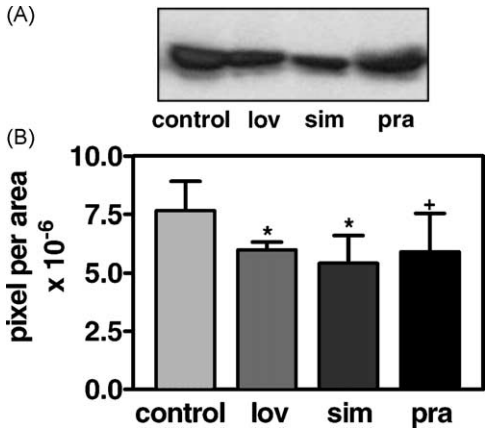

Fig. 4. Expression of the raft marker protein flotillin in SPM of control and statin-treated mice. (A) The expression of the raft marker protein flotillin in SPM of control and statin-treated C57BL/6J mice was determined using SDS–PAGE and Western blotting analysis as shown in a representative blot (refer to Section 2). lov, lovastatin; sim, simvastatin; pra, pravastatin. (B) Semi-quantitative analysis of flotillin expression was performed using the Kodak DC1C and the GraphPad 3.0 software package. Data are means ± SD (N = 5–6). (∗) $P < 0.05$ significant vs. control, (+) $P = 0.07$ as compared with control (ANOVA).

treatment (data not shown), confirming earlier studies [45]. However, DPH total anisotropy values are significantly correlated with SPM free cholesterol levels (data not shown).

3.5. Statin effects on pyrene bulk fluorescence

Pyrene is used as membrane probe to label membrane bulk fluidity [50]. Very interestingly, the hydrophilic statin pravastatin induces a significant decrease in pyrene bulk fluorescence values and thereby alters lateral membrane properties in SPM (Fig. 3A and B). A similar effect is observed for lovastatin (Fig. 3), confirming earlier results from our laboratory [45]. These findings imply that pyrene is less accessible to form excimers in SPM of lovastatin- and pravastatin-treated mice. Surprisingly, simvastatin treatment does not affect pyrene excimer formation in SPM (Fig. 3). Pyrene bulk fluorescence values of simvastatin-treated mice nearly reach control level (Fig. 3A and B).

Interestingly, lovastatin and pravastatin that significantly reduce exofacial SPM cholesterol levels (Fig. 1B) strongly decrease pyrene excimer formation in SPM (Fig. 3). Thereby, exofacial SPM cholesterol content is significantly correlated with pyrene bulk fluorescence levels (inlet Fig. 3B), whereas no such correlation is evident for the cytofacial SPM cholesterol levels (data not shown).

3.6. Statin effects on flotillin expression

Membrane lipid raft domains probably build up coalescent units in the exofacial bilayer leaflet [70,71]. Lipid rafts are possibly involved in cellular amyloidogenesis [27–29,70,71]. Expression of the raft marker protein flotillin [64] in SPM is strongly decreased by all three statins (Fig. 4A and B).

Table 2
Effects of MβCD and its cholesterol inclusion complexes on transbilayer cholesterol distribution in SPM of mice

	Percent cholesterol cytofacial	Percent cholesterol exofacial	Q (percent cholesterol exofacial/cytofacial)
Control	72.05 ± 2.99	27.95 ± 2.99	0.412 ± 0.094
CHOL−	79.42 ± 6.88	20.58 ± 6.88*	0.267 ± 0.110*
CHOL+	63.61 ± 11.49	36.39 ± 11.49^{+}	0.725 ± 0.142*

Percental cholesterol distribution of the cytofacial and exofacial leaflet was determined in SPM of control, cholesterol-depleted (CHOL−) and cholesterol-enriched (CHOL+) NMRI mice. Cholesterol depletion was performed using MβCD, cholesterol enrichment was performed using MβCD–cholesterol complexes. Synaptosomes were labelled according to the TNBS-quenching technique. Native SPM cholesterol was exchanged by SUV-incorporated DHE (refer to Section 2). Data are means ± SD (N = 4–5). (∗) $P < 0.05$ significant vs. control value of the same leaflet, (+) $P = 0.15$ as compared with control value of the same leaflet (ANOVA).

The ratio values of exofacial and cytofacial leaflet cholesterol were calculated for each group of treatment. Data are means ± SD (N = 4–5). (∗) $P < 0.05$ significant vs. control ratio (t-test).

3.7. Effects of MβCD and its cholesterol inclusion complexes on SPM transbilayer cholesterol distribution

MβCD treatment *in vitro* significantly lowers SPM free cholesterol levels. Reversely, *in vitro* treatment using cholesterol inclusion complexes significantly enhances cholesterol content in SPM. The respective free cholesterol levels (means ± SD, N = 4–5) are given as: 221.70 ± 31.98 (control), 186.20 ± 17.57* (depletion), 265.10 ± 25.06* (enrichment); $^{*}P < 0.05$ significant vs. control (t-test).

Interestingly, MβCD treatment results in significantly reduced exofacial percent cholesterol values compared to controls (Table 2), which is further expressed in decreased exofacial to cytofacial cholesterol ratio values (Table 2). Thus, MβCD exclusively extracts exofacial membrane cholesterol pools. Reversely, cholesterol enrichment with MβCD–cholesterol complexes induces contrarious effects. Percent exofacial cholesterol levels in the enrichment group are clearly enhanced compared to controls (Table 2, $^{+}P = 0.15$, t-test). Accordingly, exofacial to cytofacial cholesterol ratio values are significantly increased (Table 2). Thus, exofacial membrane cholesterol pools are most sensitive to external cholesterol manipulations using MβCD–cholesterol complexes.

4. Discussion

In view of the possible beneficial role of statins in AD, we report for the first time that lovastatin, simvastatin and pravastatin affect membranous cholesterol homeostasis in the brain, although in somewhat different manners. Consistent with our recent findings [45], lovastatin as well as

simvastatin significantly lowered the levels of unesterfied cholesterol in SPM, whereas cholesterol reduction was not significant with the hydrophilic pravastatin. Interestingly, total SPM cholesterol levels remained unaffected in all three groups. Accordingly, cholesterol ester levels were slightly enhanced in the lovastatin and simvastatin group. As pravastatin was ineffective, this probably represents a central effect of lovastatin and simvastatin. Our findings imply that (1) lovastatin and simvastatin shuttle free plasma membrane cholesterol to the cholesterol ester pool possibly via an ER cycling route [39] (Fig. 6) and that (2) net cholesterol balance across the membrane remains unchanged under statin treatment as cholesterol and its esters build up a dynamic equilibrium [39,40]. Simvastatin and pravastatin were previously shown to differentially affect cholesterol esterfication rate in AcLDL-loaded macrophages via an isoprenoid-mediated pathway [72]. Further investigations have to clarify whether the lovastatin- and simvastatin-induced cholesterol ester shifting in SPM is also sensitive for the intracellular cholesterol ester pool that was recently found to be coupled with cellular Aβ generation [44].

Recent findings indicate that excessive cellular Aβ genesis in AD is probably linked to disturbances in subcellular cholesterol compartmentation and domain sorting rather than to cellular bulk cholesterol levels [42,73,74].

Concomitantly, total membrane cholesterol levels in distinct brain regions of AD patients are not changed to any relevant degree [8,9,75]. The possible relevance of cholesterol compartmentation within the plasma membrane in AD is underlined by findings that the cholesterol content within the exofacial leaflet of SPM isolated from brains of knock-in mice carrying the human ApoE 4 allele is significantly higher compared to wild-type animals [48]. Moreover, SPM isolated from ApoE knock-out mice exhibit a similar change in exofacial cholesterol levels [76].

All three statins affected transbilayer cholesterol distribution in SPM, although in different patterns. While the hydrophilic pravastatin only affected the exofacial leaflet, the more lipophilic compounds also modulated the cytofacial membrane layer. If the latter effect is connected with the change of the cholesterol esterfication rate is not known. So far it is unclear how the statins exert these effects in the brain, especially since the hydrophilic pravastatin does not cross the BBB [22]. It might be speculated that the final central effects are initiated indirectly at the BBB micro vessel wall [34–36,77,78], e.g. by a ''cholesterol-independent'' up-regulation of endothelial NOs [34–36]. This hypothesis is strengthened by the fact that AD is often accompanied by vascular pathology and shares some common risk factors with VD [77–80]. NO is discussed to be a second messenger system of statins [81], which is additionally coupled to ApoE metabolism [82]. As lipoprotein receptors are present at the BBB [83], statin-induced signalling cascades in the endothelium of brain capillaries may subsequently alter receptor-mediated ApoE lipoprotein metabolism that possibly functions as a secondary signal transduction system [24,45,84,85].

Despite the modulation of membranous cholesterol distribution, none of the statin compounds influenced membrane microenvironment at level of DPH anisotropy in our studies, confirming earlier findings that statins affect cholesterol pools which are insensitive to DPH [45]. Intramembranous DPH flexibility might predominantly be determined by structural non-raft cholesterol pools that possibly remained unaffected by statin treatment (Fig. 5A).

In contrast, pyrene bulk fluorescence seems to be highly sensitive to statin-induced membrane alterations [45]. Pyrene measurements are based on the collision of two molecules that diffuse within the membrane [63]. Thereby it is yet not clear whether the ability for lateral diffusion and/or the possibility to form localised pyrene aggregates represents the rate-determining step for pyrene excimer formation [65]. In both cases the likelihood for excimer formation within the membrane is probably enhanced under conditions where monomeric pyrene is sterically concentrated, i.e. due to increased membrane cholesterol loading with age [50]. Statin-induced membrane cholesterol alterations probably have a differential impact on the membrane parameters sensitive to DPH and pyrene [45]. We report that pyrene bulk fluorescence was significantly diminished in lovastatin- and pravastatin-, but not in simvastatin-treated mice. As only the two former compounds significantly lowered exofacial SPM cholesterol, pyrene bulk fluorescence might be especially sensitive for cholesterol in the exofacial membrane leaflet. This hypothesis is corroborated by the finding that exofacial SPM membrane cholesterol levels significantly correlated with pyrene bulk fluorescence values. Accordingly, as exofacial membrane cholesterol content increases with age [51], SPM of aged mice consistently show enhanced pyrene bulk fluorescence values when compared to young mice [50].

Several studies reported that the *in vitro* effects of statins on APP processing could be mimicked by MβCD. MβCD is reported to diminish cellular cholesterol and Aβ load, and to affect raft assembly and structure [2–4,86,87]. Reversely, treatment of cells with MβCD–cholesterol complexes resulted in enhanced cellular bulk cholesterol and Aβ levels [2–4]. Our data clearly indicates that MβCD and its cholesterol inclusion complexes alter the transbilayer distribution of cholesterol in SPM in a contrary manner. As MβCD reduced the exofacial cholesterol pool, it probably shifts raft-associated APP cleavage to the non-amyloidogenic pathway [27–29]. MβCD–cholesterol complexes contrary enhanced exofacial cholesterol load in SPM and thereby might direct the amyloidogenic processing of APP into raft domains. Thus, MβCD and several statins not only share the pharmacological capability to reduce cellular Aβ load, but also to discretely influence membrane transbilayer distribution of cholesterol, which might thus be crucial for intracellular Aβ production (Fig. 6).

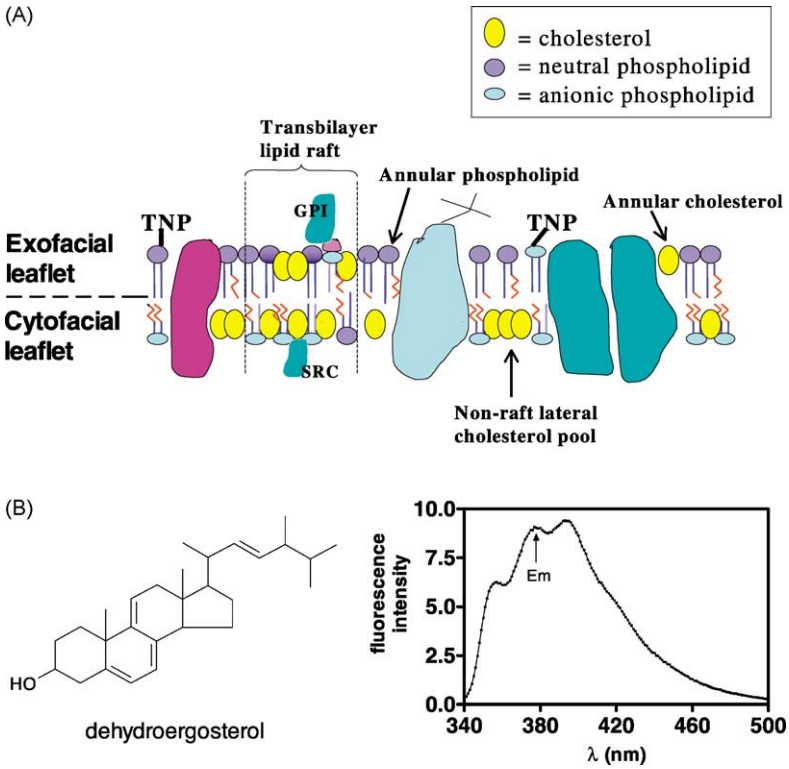

Fig. 5. Plasma membrane micro-domains and DHE fluorescence quenching. (A) Descriptive illustration of plasma membrane cholesterol distribution according to [69]. Cholesterol is enriched in the cytofacial membrane leaflet and builds up functional domains like transbilayer lipid rafts or non-raft lateral pools. Raft domains are associated with distinct signalling proteins like cytofacial src-kinase (SRC) or exofacial GPI-anchored proteins (GPI). Anionic phospholipids with unsaturated fatty acyl chains are predominantly localised in the cytofacial leaflet, neutral phospholipids with saturated fatty acids are enriched in the outer membrane leaflet. Transmembrane proteins are embedded in the bilayer and surrounded by annular lipids. Determination of the transbilayer distribution of cholesterol requires a trinitrophenylation reaction using TNBS in SPM conducted at 4°. TNBS covalently links primary amino moieties of phospholipids in the exofacial leaflet (TNP: trinitrophenyl-residues) and does not penetrate the membrane core region. SUV-incorporated DHE exchanges with native membrane cholesterol in both leaflets in an equilibrium manner [51]. Fluorescence emission of excited DHE located in the exofacial leaflet is quenched by TNBS. Thus, DHE fluorescence of the labelled sample refers to the cholesterol content in the cytofacial leaflet. The DHE fluorescence signal of the unlabelled sample refers to bulk cholesterol levels in SPM. The difference between these signals represents the exofacial cholesterol content. (B) Chemical structure and fluorescence emission spectrum of DHE in SUV. The fluorophore region is excited at 324 nm, emission (Em) is recorded at 375 nm.

High levels of exofacial raft cholesterol are suspected to provide an excellent environment for intra-membranous amyloidogenic APP cleavage by β- and γ-secretases and hence may enhance this important pathogenetic process in AD [27–29,70,88]. Recent findings using Asp-2-transfected 293 cells point out that increasing intracellular cholesterol levels lead to the localisation of the β-secretase Asp-2 enzyme into cholesterol-rich membrane micro-domains, while lovastatin treatment causes a more diffuse enzyme localisation and thereby probably disperses β-secretase from its substrate APP [89]. Some evidence indicates that the PM non-raft cholesterol pool primarily senses the amount of cellular bulk cholesterol [40]. Raft destruction, e.g. with sphingomyelinase shuttles cholesterol into the non-raft pool, which probably flows back to the ER and thus blocks intracellular SREBP/SCAP translocation to the Golgi and further cholesterol synthesis (Fig. 6) [40,90].

Interestingly, all three statin compounds in our studies lowered the expression of flotillin, a widely used lipid raft marker protein [64,86]. Again, as pravastatin is active, the mechanism might be indirect. Although no purified raft fractions from SPM were isolated due to the limitation of available tissue, this finding points to specific statin-induced alterations in raft structure and distribution. Recently, inhibition of caveolin expression in the presence of statins has been demonstrated in endothelial cells, resulting in an up-regulation of NO release [91].

In conclusion, statins directly and/or indirectly exert various effects on membrane cholesterol homeostasis in the central nervous system. Statin-induced disturbances in the equilibrium of exofacial raft cholesterol and cytofacial non-raft cholesterol may subsequently change the accessibility of membrane cholesterol pools to the ER sensor and ACAT [92] as well as to raft-associated proteins like secretases [26–28] or APP (Fig. 6) [71,88], which might secondary shift cellular metabolism towards the non-amyloidogenic pathway. According to this hypothesis, further investigations have to clarify whether brain membrane cholesterol and raft distribution are altered during AD.

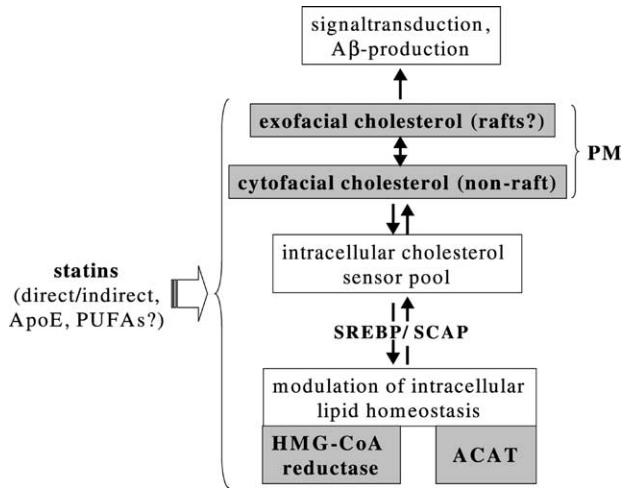

Fig. 6. Putative cellular targets of statins and secondary effects on intracellular cholesterol homeostasis. Statins directly or indirectly induce alterations in the equilibrium of transbilayer cholesterol distribution in the plasma membrane and thereby affect the accessibility of membrane cholesterol to distinct cellular domains. Exofacial raft cholesterol reveals to be crucial for membranous signal transduction processes and probably cellular Aβ production from its precursor APP. Cytofacial cholesterol in non-raft pools might act as a sensor domain which can cycle back to the ER and thus influence intracellular lipid homeostasis and distribution via the SREBP/SCAP pathway and other feedback cascades like metabolic control of HMG-CoA reductase or ACAT activity.

Acknowledgments

This study was supported by the Hanna Bragard Foundation. The excellent technical assistance by Andrea Wilke, Claudia Jourdan, Kristina Treiber, Gisela Holoubek and Sebastian Schaffer is gratefully acknowledged.

References

[1] Roher AE, Kuo YM, Kokjohn KM, Emmerling MR, Gracon S. Amyloid and lipids in the pathology of Alzheimer disease. Amyloid 1999;6:136–45.
[2] Frears ER, Stephens DJ, Walters CE, Davies H, Austen BM. The role of cholesterol in the biosynthesis of beta-amyloid. Neuroreport 1999; 10:1699–705.
[3] Bodovitz S, Klein WL. Cholesterol modulates alpha-secretase cleavage of amyloid precursor protein. J Biol Chem 1996;271: 4436–40.
[4] Fassbender K, Simons M, Bergmann C, Stroick M, Lutjohann D, Keller P, Runz H, Kuhl S, Bertsch T, von Bergmann K, Hennerici M, Beyreuther K, Hartmann T. Simvastatin strongly reduces levels of Alzheimer's disease beta-amyloid peptides Abeta 42 and Abeta 40 *in vitro* and *in vivo*. Proc Natl Acad Sci USA 2001;98:5856–61.
[5] Wood WG, Schroeder F, Avdulov NA, Chochina SV, Igbavboa U. Recent advances in brain cholesterol dynamics: transport, domains, and Alzheimer's disease. Lipids 1999;34:225–34.
[6] Simons M, Keller P, De Strooper B, Beyreuther K, Dotti CG, Simons K. Cholesterol depletion inhibits the generation of beta-amyloid in hippocampal neurons. Proc Natl Acad Sci USA 1998;95:6460–4.
[7] Czech C, Forstl H, Hentschel F, Monning U, Besthorn C, Geiger-Kabisch C, Sattel H, Masters C, Beyreuther K. Apolipoprotein E-4 gene dose in clinically diagnosed Alzheimer's disease: prevalence, plasma cholesterol levels and cerebrovascular change. Eur Arch Psychiatr Clin Neurosci 1994;243:291–2.
[8] Svennerholm L, Gottfries CG. Membrane lipids, selectively diminished in Alzheimer brains, suggest synapse loss as a primary event in early-onset form (type I) and demyelination in late-onset form (type II). J Neurochem 1994;62:1039–47.
[9] Mason RP, Shoemaker WJ, Shajenko L, Chambers TE, Herbette LG. Evidence for changes in the Alzheimer's disease brain cortical membrane structure mediated by cholesterol. Neurobiol Aging 1992;13: 413–9.
[10] Kakio A, Nishimoto SS, Yanagisawa K, Kozutsumi Y, Matsuzaki K. Cholesterol-dependent formation of GM1 ganglioside-bound amyloid beta-protein, an endogenous seed for Alzheimer amyloid. J Biol Chem 2001;276:24985–90.
[11] Selkoe DJ. Alzheimer's disease: a central role for amyloid. J Neuropathol Exp Neurol 1994;53:438–47.
[12] Bayer TA, Wirths O, Majtenyi K, Hartmann T, Multhaup G, Beyreuther K, Czech C. Key factors in Alzheimer's disease: beta-amyloid precursor protein processing, metabolism and intraneuronal transport. Brain Pathol 2001;11:1–11.
[13] Hartmann H, Eckert A, Muller WE. beta-Amyloid protein amplifies calcium signalling in central neurons from the adult mouse. Biochem Biophys Res Commun 1993;194:1216–20.
[14] Kawahara M, Kuroda Y. Molecular mechanism of neurodegeneration induced by Alzheimer's beta-amyloid protein: channel formation and disruption of calcium homeostasis. Brain Res Bull 2000;53: 389–97.
[15] Müller WE, Kirsch C, Eckert GP. Membrane-disordering effects of beta-amyloid peptides. Biochem Soc Trans 2001;29:617–23.
[16] Lousberg TR, Denham AM, Rasmussen JR. A comparison of clinical outcome studies among cholesterol-lowering agents. Ann Pharmacother 2001;35:1599–607.
[17] Wolozin B, Kellman W, Rousseau P, Celesia GG, Siegel G. Decreased prevalence of Alzheimer disease associated with 3-hydroxy-3-methyglutaryl coenzyme A reductase inhibitors. Arch Neurol 2000;57: 1439–43.
[18] Jick H, Zornberg GL, Jick SS, Seshadri S, Drachman DA. Statins and the risk of dementia. Lancet 2000;356:1627–31.
[19] Hamelin BA, Turgeon J. Hydrophilicity/lipophilicity: relevance for the pharmacology and clinical effects of HMG-CoA reductase inhibitors. Trends Pharmacol Sci 1998;19:26–37.
[20] Guillot F, Misslin P, Lemaire M. Comparison of fluvastatin and lovastatin blood–brain barrier transfer using *in vitro* and *in vivo* methods. J Cardiovasc Pharmacol 1993;21:339–46.
[21] Saheki A, Terasaki T, Tamai I, Tsuji A. *In vivo* and *in vitro* blood–brain barrier transport of 3-hydroxy-3-methylglutaryl coenzyme A (HMG-CoA) reductase inhibitors. Pharm Res 1994;11:305–11.
[22] Botti RE, Triscari J, Pan HY, Zayat J. Concentrations of pravastatin and lovastatin in cerebrospinal fluid in healthy subjects. Clin Neuropharmacol 1991;14:256–61.
[23] Komai T, Shigehara E, Tokui T, Koga T, Ishigami M, Kuroiwa C, Horiuchi S. Carrier-mediated uptake of pravastatin by rat hepatocytes in primary culture. Biochem Pharmacol 1992;43:667–70.
[24] Dietschy JM, Turley SD. Cholesterol metabolism in the brain. Curr Opin Lipidol 2001;12:105–12.
[25] Hartmann T. Cholesterol, A beta and Alzheimer's disease. Trends Neurosci 2001;24:S45–8.
[26] Kojro E, Gimpl G, Lammich S, Marz W, Fahrenholz F. Low cholesterol stimulates the nonamyloidogenic pathway by its effect on the alpha-secretase ADAM 10. Proc Natl Acad Sci USA 2001;98: 5815–20.
[27] Marx J. Alzheimer's disease: bad for the heart, bad for the mind? Science 2001;294:508–9.
[28] Golde TE, Eckman CB. Cholesterol modulation as an emerging strategy for the treatment of Alzheimer's disease. Drug Discov Today 2001;6:1049–55.

[29] Wolozin B. A fluid connection: cholesterol and A beta. Proc Natl Acad Sci USA 2001;98:5371–3.
[30] Refolo LM, Pappolla MA, LaFrancois J, Malester B, Schmidt SD, Thomas-Bryant T, Tint GS, Wang R, Mercken M, Petanceska SS, Duff KE. A Cholesterol-lowering drug reduces beta-amyloid pathology in a transgenic mouse model of Alzheimer's disease. Neurobiol Dis 2001; 8:890–9.
[31] Shie FS, Jin LW, Cook DG, Leverenz JB, LeBoeuf RC. Diet-induced hypercholesterolemia enhances brain Abeta accumulation in transgenic mice. Neuroreport 2002;13:455–9.
[32] Doggrell SA. Statins in the 21st century: end of the simple story? Expert Opin Invest Drugs 2001;10:1755–66.
[33] Desager JP, Horsmans Y. Clinical pharmacocinetics of 3-hydroxy-3-methylglutaryl-coenzyme A reductase inhibitors. Clin Pharmacokinet 1996;31:348–71.
[34] Bellosta S, Ferri N, Bernini F, Paoletti R, Corsini A. Non-lipid-related effects of statins. Ann Med 2000;32:164–76.
[35] Takemoto M, Liao JK. Pleiotropic effects of 3-hydroxy-3-methylglutaryl coenzyme a reductase inhibitors. Arterioscler Thromb Vasc Biol 2001;21:1712–9.
[36] Corsini A, Bernini F, Quarato P, Donetti E, Bellosta S, Fumagalli R, Paoletti R, Soma VM. Non-lipid-related effects of 3-hydroxy-3-methylglutaryl coenzyme A reductase inhibitors. Cardiology 1996; 87:458–68.
[37] Cucchiara B, Kasner SE. Use of statins in CNS disorders. J Neurol Sci 2001;187:81–9.
[38] Bonetta L. Potential neurological value of statins increases. Nat Med 2002;8:541.
[39] Liscum L, Dahl NK. Intracellular cholesterol transport. J Lipid Res 1992;33:1239–54.
[40] Simons K, Ikonen E. How cells handle cholesterol. Science 2000; 290:1721–6.
[41] Schroeder F, Woodford JK, Kavecansky J, Wood WG, Joiner C. Cholesterol domains in biological membranes. Mol Membr Biol 1995;12:113–9.
[42] Runz H, Rietdorf J, Tomic I, de Bernard M, Beyreuther K, Pepperkok R, Hartmann T. Inhibition of intracellular cholesterol transport alters presenilin localization and amyloid precursor protein processing in neuronal cells. J Neurosci 2002;22:1679–89.
[43] Liu Y, Peterson DA, Schubert D. Amyloid beta peptide alters intracellular vesicle trafficking and cholesterol homeostasis. Proc Natl Acad Sci USA 1998;95:13266–71.
[44] Puglielli L, Konopka G, Pack-Chung E, Ingano LA, Berezovska O, Hyman BT, Chang TY, Tanzi RE, Kovacs DM. Acyl-coenzyme A: cholesterol acyltransferase modulates the generation of the amyloid beta-peptide. Nat Cell Biol 2001;3:905–12.
[45] Eckert GP, Kirsch C, Mueller WE. Differential effects of lovastatin treatment on brain cholesterol levels in normal and apoE-deficient mice. Neuroreport 2001;12:883–7.
[46] Locatelli S, Lutjohann D, Schmidt HH, Otto C, Beisiegel U, von Bergmann K. Reduction of plasma 24*S*-hydroxycholesterol (cerebrosterol) levels using high-dosage simvastatin in patients with hypercholesterolemia: evidence that simvastatin affects cholesterol metabolism in the human brain. Arch Neurol 2002;59:213–6.
[47] Bjorkhem I, Lutjohann D, Diczfalusy U, Stahle L, Ahlborg G, Wahren J. Cholesterol homeostasis in human brain: turnover of 24*S*-hydroxycholesterol and evidence for a cerebral origin of most of this oxysterol in the circulation. J Lipid Res 1998;39: 1594–600.
[48] Hayashi H, Igbavboa U, Hamanaka H, Kobayashi M, Fujita SC, Wood WG, Yanagisawa K. Cholesterol is increased in the exofacial leaflet of synaptic plasma membranes of human apolipoprotein E4 knock-in mice. Neuroreport 2002;13:383–6.
[49] Cardenas-Vazquez JCR, Martinez FMA. Comparative toxicity of high doses of vastatins currently used by clinicians, in CD-1 male mice fed with a hypercholesterolemic diet. Life Sci 1999;65:947–56.
[50] Eckert GP, Wood WG, Muller WE. Effects of aging and beta-amyloid on the properties of brain synaptic and mitochondrial membranes. J Neural Transm 2001;108:1051–64.
[51] Igbavboa U, Avdulov NA, Schroeder F, Wood WG. Increasing age alters transbilayer fluidity and cholesterol asymmetry in synaptic plasma membranes of mice. J Neurochem 1996;66:1717–25.
[52] Schroeder F, Nemecz G, Wood WG, Joiner C, Morrot G, Ayraut-Jarrier M, Devaux PF. Transmembrane distribution of sterol in the human erythrocyte. Biochim Biophys Acta 1991;1066:183–92.
[53] Schmalzing G, Kutschera P. Modulation of ATPase activities of human erythrocyte membranes by free fatty acids or phospholipase A2. J Membr Biol 1982;69:65–76.
[54] Schroeder F, Frolov AA, Murphy EJ, Atshaves BP, Jefferson JR, Pu L, Wood WG, Foxworth WB, Kier AB. Recent advances in membrane cholesterol domain dynamics and intracellular cholesterol trafficking. Proc Soc Exp Biol Med 1996;213:150–77.
[55] Lowry OH, Rosebrough NJ, Farr AL, Randall RJ. Protein measurement with the Folin phenol reagent. J Biol Chem 1951;193:265–75.
[56] Schroeder F, Morrison WJ, Gorka C, Wood WG. Transbilayer effects of ethanol on fluidity of brain membrane leaflets. Biochim Biophys Acta 1988;946:85–94.
[57] Kaiser RD, London E. Location of diphenylhexatriene (DPH) and its derivatives within membranes: comparison of different fluorescence quenching analyses of membrane depth. Biochemistry 1998;37: 8180–90.
[58] Lentz BR. Use of fluorescent probes to monitor molecular order and motions within liposome bilayers. Chem Phys Lipids 1993;64: 99–116.
[59] Weber G. Resolution of heterogeneous fluorescence from proteins and aromatic amino acids by phase-sensitive detection of fluorescence. Biochem J 1952;51:145–67.
[60] Sweet WD, Schroeder F. Plasma membrane lipid composition modulates action of anesthetics. Biochim Biophys Acta 1986;861:53–61.
[61] Sweet WD, Schroeder F. Charged anaesthetics alter LM-fibroblast plasma-membrane enzymes by selective fluidization of inner or outer membrane leaflets. Biochem J 1986;239:301–10.
[62] Mulders F, van Langen H, van Ginkel G, Levine YK. Effects of steroid molecules on the dynamical structure of dioleoylphosphatidylcholine and digalactosyldiacylglycerol bilayers. Biochim Biophys Acta 1986; 859:209–18.
[63] Macdonald AG, Wahle KW, Cossins AR, Behan MK. Temperature, pressure and cholesterol effects on bilayer fluidity a comparison of pyrene excimer/monomer ratios with the steady-state fluorescence polarization of diphenylhexatriene in liposomes and microsomes. Biochim Biophys Acta 1988;938:231–42.
[64] Eckert GP, Igbavboa U, Müller WE, Wood WG. Lipid rafts of purified mouse brain synaptosomes prepared with or without detergent reveal different lipid and protein domains. Brain Res 2002; in press.
[65] Kirsch C, Eckert GP, Müller WE. Cholesterol attenuates the membrane perturbing properties of β-amyloid peptides. Amyloid 2002; 9:149–59.
[66] Auerbach BJ, Parks JS, Applebaum-Bowden D. A rapid and sensitive micro-assay for the enzymatic determination of plasma and lipoprotein cholesterol. J Lipid Res 1990;31:738–42.
[67] Chalvardjian A, Rudnicki E. Determination of lipid phosphorus in the nanomolar range. Anal Biochem 1970;36:225–6.
[68] Krause BR, Princen HM. Lack of predictability of classical animal models for hypolipidemic activity: a good time for mice? Atherosclerosis 1998;140:15–24.
[69] Schroeder F, Gallegos AM, Atshaves BP, Storey SM, McIntosh AL, Petrescu AD, Huang H, Starodub O, Chao H, Yang H, Frolov A, Kier AB. Recent advances in membrane microdomains: rafts, caveolae, and intracellular cholesterol trafficking. Exp Biol Med (Maywood) 2001; 226:873–90.
[70] Simons K, Toomre D. Lipid rafts and signal transduction. Nat Rev Mol Cell Biol 2000;1:31–9.

[71] Riddell DR, Christie G, Hussain I, Dingwall C. Compartmentalization of beta-secretase (Asp2) into low-buoyant density, noncaveolar lipid rafts. Curr Biol 2001;11:1288–93.
[72] Bernini F, Didoni G, Bonfadini G, Bellosta S, Fumagalli R. Requirement for mevalonate in acetylated LDL induction of cholesterol esterification in macrophages. Atherosclerosis 1993;104: 19–26.
[73] Yamazaki T, Chang TY, Haass C, Ihara Y. Accumulation and aggregation of amyloid beta-protein in late endosomes of Niemann-pick type C cells. J Biol Chem 2001;276:4454–60.
[74] Wood WG, Eckert GP, Igbavboa U, Müller WE. Amyloid beta-peptide interactions with membranes and cholesterol: causes and causalities of Alzheimer's disease. Biochim Biophys Acta 2002; in press.
[75] Eckert GP, Cairns NJ, Maras A, Gattaz WF, Muller WE. Cholesterol modulates the membrane-disordering effects of beta-amyloid peptides in the hippocampus: specific changes in Alzheimer's disease. Dement Geriatr Cogn Disord 2000;11:181–6.
[76] Igbavboa U, Avdulov NA, Chochina SV, Wood WG. Transbilayer distribution of cholesterol is modified in brain synaptic plasma membranes of knockout mice deficient in the low-density lipoprotein receptor, apolipoprotein E, or both proteins. J Neurochem 1997;69: 1661–7.
[77] Skoog I. Vascular aspects in Alzheimer's disease. J Neural Transm Suppl 2000;59:37–43.
[78] Endres M, Laufs U, Huang Z, Nakamura T, Huang P, Moskowitz MA, Liao JK. Stroke protection by 3-hydroxy-3-methylglutaryl (HMG)-CoA reductase inhibitors mediated by endothelial nitric oxide synthase. Proc Natl Acad Sci USA 1998;95:8880–5.
[79] Kivipelto M, Helkala EL, Laakso MP, Hanninen T, Hallikainen M, Alhainen K, Soininen H, Tuomilehto J, Nissinen A. Midlife vascular risk factors and Alzheimer's disease in later life: longitudinal, population based study. Br Med J 2001;322:1447–51.
[80] Kalaria RN, Ballard C. Overlap between pathology of Alzheimer disease and vascular dementia. Alzheimer Dis Assoc Disord 1999; 13(Suppl 3):S115–23.
[81] Das UN. Essential fatty acids as possible mediators of the actions of statins. Prostaglandins Leukot Essent Fatty Acids 2001;65:37–40.
[82] Colton CA, Brown CM, Czapiga M, Vitek MP. Apolipoprotein-E allele-specific regulation of nitric oxide production. Ann NY Acad Sci 2002;962:212–25.
[83] Meresse S, Delbart C, Fruchart JC, Cecchelli R. Low-density lipoprotein receptor on endothelium of brain capillaries. J Neurochem 1989;53:340–5.
[84] Wolozin B. Cholesterol and Alzheimer's disease. Biochem Soc Trans 2002;30:525–9.
[85] Igbavboa U, Hamilton J, Kim HY, Sun GY, Wood WG. A new role for apolipoprotein E: modulating transport of polyunsaturated phospholipid molecular species in synaptic plasma membranes. J Neurochem 2002;80:255–61.
[86] Kabouridis PS, Janzen J, Magee AL, Ley SC. Cholesterol depletion disrupts lipid rafts and modulates the activity of multiple signaling pathways in T lymphocytes. Eur J Immunol 2000;30:954–63.
[87] Hao M, Mukherjee S, Maxfield FR. Cholesterol depletion induces large scale domain segregation in living cell membranes. Proc Natl Acad Sci USA 2001;98:13072–7.
[88] Wahrle S, Das P, Nyborg AC, McLendon C, Shoji M, Kawarabayashi T, Younkin LH, Younkin SG, Golde TE. Cholesterol-dependent gamma-secretase activity in buoyant cholesterol-rich membrane microdomains. Neurobiol Dis 2002;9:11–23.
[89] Sidera C, Frimpong-Manso J, Liu C, Austen BM. The role of cholesterol in the processing of beta-secretase Asp-2. In: Korczyn AD, editor. Proceedings of the 2nd International Congress on Vascular Dementia, Salzburg, Austria. Monduzzi Editore, International Proceedings Division; 2002. p. 147–53.
[90] Slotte JP. Cholesterol–sphingomyelin interactions in cells—effects on lipid metabolism. Subcell Biochem 1997;28:277–93.
[91] Feron O, Dessy C, Desager JP, Balligand JL. Hydroxy-methylglutaryl-coenzyme A reductase inhibition promotes endothelial nitric oxide synthase activation through a decrease in caveolin abundance. Circulation 2001;103:113–8.
[92] Accad M, Smith SJ, Newland DL, Sanan DA, King Jr LE, Linton MF, Fazio S. Massive xanthomatosis and altered composition of atherosclerotic lesions in hyperlipidemic mice lacking acyl CoA:cholesterol acyltransferase 1. J Clin Invest 2000;105:711–9.